

Manuscript Number: PROTIS-D-16-00074R3

Title: Variation in basal body localisation and targeting of trypanosome RP2 and FOR20 proteins

Article Type: Original Paper

Keywords: basal body; ciliogenesis; FOP; protein targeting; Trypanosoma brucei; YL1/2

Corresponding Author: Professor Michael L. Ginger, PhD

Corresponding Author's Institution: University of Huddersfield

First Author: Jane Harmer

Order of Authors: Jane Harmer; Xin Qi; Gabriella Toniolo; Aysha Patel; Hannah Shaw; Fiona E Benson; Michael L. Ginger, PhD; Paul G McKean

Abstract: TOF-LisH-PLL motifs defines FOP family proteins; some members are involved in flagellum assembly. The critical role of FOP family protein FOR20 is poorly understood. Here, we report relative localisations of the four FOP family proteins in parasitic Trypanosoma brucei: TbRP2, TbOFD1 and TbFOP/FOP1-like are mature basal body proteins whereas TbFOR20 is present on pro- and mature basal bodies - on the latter it localises distal to TbRP2. We discuss how the data, together with published work for another protist Giardia intestinalis, informs on likely FOR20 function. Moreover, our localisation study provides convincing evidence that the antigen recognised by monoclonal antibody YL1/2 at trypanosome mature basal bodies is FOP family protein TbRP2, not tyrosinated  $\alpha$ -tubulin as widely stated in the literature. Curiously, FOR20 proteins from T. brucei and closely related African trypanosomes possess short, negatively-charged N-terminal extensions absent from FOR20 in other trypanosomatids and other eukaryotes. The extension is necessary for protein targeting, but insufficient to re-direct TbRP2 to probasal bodies. Yet, FOR20 from the American trypanosome T. cruzi, which lacks any extension, localises to pro- and mature basal bodies when expressed in T. brucei. This identifies unexpected variation in FOR20 architecture that is presently unique to one clade of trypanosomatids.

# Variation in basal body localisation and targeting of trypanosome RP2 and FOR20 proteins

Jane Harmer<sup>a</sup>, Xin Qi<sup>a</sup>, Gabriella Toniolo<sup>a</sup>, Aysha Patel<sup>a</sup>, Hannah Shaw<sup>a</sup>, Fiona E. Benson<sup>a</sup>, Michael L. Ginger<sup>b,1</sup>, and Paul G. McKean<sup>a,1</sup>

<sup>a</sup>Faculty of Health and Medicine, Division of Biomedical and Life Sciences, Lancaster University, Lancaster LA1 4YQ, UK.

<sup>b</sup>Department of Biological Sciences, School of Applied Sciences, University of Huddersfield, Queensgate, Huddersfield, HD1 3DH, UK.

<sup>1</sup>Co-senior and co-corresponding authors: [M.Ginger@hud.ac.uk](mailto:M.Ginger@hud.ac.uk); [p.mckean@lancaster.ac.uk](mailto:p.mckean@lancaster.ac.uk)

TOF-LisH-PLL motifs defines FOP family proteins; some members are involved in flagellum assembly. The critical role of FOP family protein FOR20 is poorly understood. Here, we report relative localisations of the four FOP family proteins in parasitic *Trypanosoma brucei*: *TbRP2*, *TbOFD1* and *TbFOP/FOP1*-like are mature basal body proteins whereas *TbFOR20* is present on pro- and mature basal bodies – on the latter it localises distal to *TbRP2*. We discuss how the data, together with published work for another protist *Giardia intestinalis*, informs on likely FOR20 function. Moreover, our localisation study provides convincing evidence that the antigen recognised by monoclonal antibody YL1/2 at trypanosome mature basal bodies is FOP family protein *TbRP2*, not tyrosinated  $\alpha$ -tubulin as widely stated in the literature. Curiously, FOR20 proteins from *T. brucei* and closely related African trypanosomes possess short, negatively-charged N-terminal extensions absent from FOR20 in other trypanosomatids and other eukaryotes. The extension is necessary for protein targeting, but insufficient to re-direct *TbRP2* to probasal bodies. Yet, FOR20 from the American trypanosome *T. cruzi*, which lacks any extension, localises to pro- and mature basal bodies when expressed in *T. brucei*. This identifies unexpected variation in FOR20 architecture that is presently unique to one clade of trypanosomatids.

**Keywords:** basal body; ciliogenesis; FOP; protein targeting; *Trypanosoma brucei*; YL1/2

**Running title:** FOP family protein targeting in trypanosomatids

## Introduction

In eukaryotic cells, cilia (or flagella) are often central to cell swimming, cell feeding, reproduction, and sensory perception. Length (cilia tend to be thought of as shorter), number (large numbers of cilia tend to be arrayed across cell surfaces whereas examples of flagellate protists with more than two flagella are fewer than taxa possessing one flagellum or two flagella), and principal mode of motion (an oar-like ciliary waveform versus more whip-like flagellar beating) are the obvious determinants commonly used for distinguishing cilia from flagella. Yet, these terms refer essentially to variants of the same organelle that have as their defining structure a microtubule axoneme (Moran et al. 2014).

43 In the classic '9+2' configuration, axonemes are composed of nine outer-doublet  
1 44 microtubules surrounding two singlet microtubules. Irrespective of the number of outer-  
2 45 doublet microtubules present (structures with as few as three outer-doublets have been  
3 46 described (Prensier et al. 2008)), axoneme elongation occurs from a barrel-shaped  
4 47 microtubule organising centre (MTOC) or centriole, which in the context of flagellum  
5 48 assembly is better described as a basal body. *De novo* basal body biogenesis is known, but  
6 49 in many organisms a probasal body, or pro-centriole, comprised of triplet microtubules,  
7 50 rather than doublets, is physically associated with a mature basal body (Fritz-Laylin et al.  
8 51 2016). Thus, in trypanosomatids, the flagellate parasitic protists featured in this work,  
9 52 probasal body-to-basal body maturation occurs when doublet microtubules extend from A-  
10 53 and B-tubules of the triplets of the probasal body, thereby forming the transition zone of the  
11 54 mature basal body (Vaughan and Gull 2015). The transition zone is capped at the distal end  
12 55 by a basal plate from which the axoneme proper subsequently extends by a process that, as  
13 56 in many other flagellate cells, is dependent upon an intraflagellar transport (IFT) system  
14 57 (Absalon et al. 2008, Davidge et al. 2006). Coincident with trypanosome probasal body  
15 58 maturation, biogenesis of two new probasal bodies and their association to either the newly  
16 59 matured basal body or the basal body matured in a previous cell cycle, also occurs  
17 60 (Vaughan and Gull 2015).

21 61 Estimates derived from the proteomics of organelles isolated from diverse taxa  
22 62 suggest 200-300 different proteins are likely to be *bona fide* components of mature basal  
23 63 bodies (and their associated appendages) e.g. (Keller et al. 2005, Kilburn et al. 2007). Such  
24 64 estimates provide an interesting contrast with bioinformatics-based comparisons that  
25 65 indicate structural conservation and complexity of centriole/basal body symmetry across the  
26 66 breadth of eukaryotic evolution may be dependent upon only a handful of conserved  
27 67 proteins (Carvalho-Santos et al. 2011, Hodges et al. 2010). One basal body/centriole protein  
28 68 conserved in evolutionarily diverse flagellate eukaryotes is FOR20.

31 69 The only recognisable architectural features of the small FOP-related protein of 20  
32 70 kDa (or FOR20) are also shared with other FOP family proteins (e.g. FOP, TONNEAU1 and  
33 71 OFD1), namely N-terminally localised TOF, LisH and 'PLL' motifs (Sedjai et al. 2010). The  
34 72 protein was initially described as present at the distal end of the basal body in the ciliate  
35 73 *Tetrahymena thermophila* (where it is known as Bbc20 (Kilburn et al. 2007)) and  
36 74 subsequently as a component of the granular pericentriolar satellites that surround the  
37 75 centrosome (a centriole-bearing MTOC) in animal cells (Fritz-Laylin and Cande 2010, Sedjai  
38 76 et al. 2010). FOR20 is required for assembly of the non-motile primary cilium that extends as  
39 77 a sensory antenna from the surface of many animal cell types (Sedjai et al. 2010). In such  
40 78 cells, primary cilium formation occurs following centrosome relocation from a normally  
41 79 central intracellular position to the cortical cytoskeleton and the maturation of the mother  
42 80 centriole to a basal body (Dawe et al. 2007) although how FOR20 contributes to primary  
43 81 cilium assembly is not certain. Experimental analysis by gene-specific RNA interference  
44 82 (RNAi) in the ciliate *Paramecium* indicates its FOR20 is a stable component of the ciliate  
45 83 basal body, rather than subject to turn over, and is required for basal body docking at the  
46 84 plasma membrane and/or transition zone maturation (Aubusson-Fleury et al. 2012). Similar  
47 85 to Bbc20 in *Tetrahymena* and consistent with a proposed role in membrane docking,  
48 86 *Paramecium* FOR20 also localises to the distal end of both older (ciliated) and their  
49 87 associated non-ciliated, younger basal bodies (Aubusson-Fleury et al. 2012).

53 88 Generally speaking, FOP family proteins are found in flagellate eukaryotes, but not in  
54 89 organisms that lack a capacity to build a flagellum – acentriolar plants are the exception to  
55 90 this rule. In each of the taxa examined thus far, the FOP protein family is small in number  
56 91 (Azimzadeh et al. 2008, Hodges et al. 2010) and among flagellates the other family  
57 92 members are also centriolar and required for flagellum assembly (André et al. 2014,  
58 93 Aubusson-Fleury et al. 2012, Sedjai et al. 2010, Singla et al. 2010). In acentriolar plant cells  
59 94 another FOP-related protein, TONNEAU1, is found; it is required for organisation of cortical

95 microtubule arrays and interacts with the classic MTOC protein centrin (Azimzadeh et al.  
1 96 2008, Spinner et al. 2010). In kinetoplastid protists (which include the parasitic  
2 97 trypanosomatids), four proteins comprise the FOP family: three conserved family members,  
3 98 FOP/FOP1-like, FOR20 and OFD1, plus a lineage-specific protein known as *TbRP2* in the  
4 99 African trypanosome *Trypanosoma brucei* (André et al. 2014). In this lineage-specific protein  
5 100 the TOF-LisH-PLL motif sequence lies, apparently uniquely, upstream of a tubulin cofactor C  
6 101 domain – although there is indication of a conserved requirement for a tubulin cofactor C  
7 102 domain-containing protein *per se* in flagellum assembly. Thus, *TbRP2* is found at mature  
8 103 basal bodies and in *T. brucei* is required for assembly of a full-length flagellum and an intact  
9 104 axoneme (André et al. 2014, Stephan et al. 2007). Intriguingly, we reported recombinant  
10 105 *TbRP2* is recognised by monoclonal antibody YL1/2 (André et al. 2014). YL1/2 is classically  
11 106 used to detect tyrosinated  $\alpha$ -tubulin in eukaryotic cells, including by many in the  
12 107 trypanosomatid community. There is no doubt that YL1/2 recognises *T. brucei* tyrosinated  $\alpha$ -  
13 108 tubulin, but likely additional recognition of *TbRP2* calls into question whether there is a  
14 109 mature basal body pool of tyrosinated  $\alpha$ -tubulin specifically recognised by YL1/2.

17  
18 110 Peculiarities of the kinetoplastid FOP family are not restricted to the presence of a  
19 111 lineage-specific family member: the only candidate orthologue of FOP, which in animal cells  
20 112 is required for ciliogenesis (Lee and Stearns 2013), is a protein we term FOP/FOP1-like and  
21 113 is required in *T. brucei* for assembly of an essential (lineage-specific) extra-axonemal  
22 114 structure, the paraflagellar rod, but has no discernible effect on axoneme assembly (André et  
23 115 al. submitted). Among African trypanosome species *FOR20* is predicted to encode a protein  
24 116 possessing a predicted short N-terminal extension not seen in either other kinetoplastids or  
25 117 other eukaryotes. Here, we demonstrate the N-terminal extension predicted for *T. brucei*  
26 118 *FOR20* is real, rather than an artefact of gene annotation, and essential but not sufficient for  
27 119 protein localisation to both pro- and mature basal bodies throughout the trypanosome cell  
28 120 cycle. Interestingly, *FOR20* from the distantly related American trypanosome *T. cruzi*, which  
29 121 lacks an N-terminal extension, is also targeted to pro- and mature basal bodies when  
30 122 expressed in *T. brucei*. Collectively, data presented here provide new insights into the  
31 123 functional diversification of the conserved, yet small FOP protein family, the spatial  
32 124 organisation of trypanosome basal body biogenesis, and provide further indication that  
33 125 *TbRP2* is the basal body antigen specifically recognised by YL1/2.

## 36 37 126 38 39 127 **Results**

### 40 41 128 *TbFOR20* is present at pro- and mature basal bodies

42  
43 129 The *T. brucei* *FOR20* orthologue is encoded by Tb927.11.3090. Expressed from an  
44 130 endogenous chromosomal locus as an N-terminal fusion with YFP, *TbFOR20* is targeted to  
45 131 both pro- and mature basal bodies, with YFP fluorescence lying distal to the indirect  
46 132 immunofluorescence signal observed using monoclonal antibody BBA4 (Fig. 1A). BBA4  
47 133 recognises an unknown trypanosome antigen from the proximal end of pro- and mature  
48 134 basal bodies (Woodward et al. 1995); thus YFP::*TbFOR20* localises to, or towards, the distal  
49 135 end of probasal bodies and is retained on mature basal bodies. In trypanosomatids, pro- and  
50 136 mature basal bodies are physically attached at their proximal ends to the mitochondrial  
51 137 genome (or kinetoplast) by a complex filament network, the tri-partite attachment complex  
52 138 (TAC), that traverses outer and inner mitochondrial membranes (Ogbadoyi et al. 2003); thus,  
53 139 the fluorescence from 6-diamidino-2-phenylindole (DAPI)-stained kinetoplasts lies proximal  
54 140 to the BBA4-immunolabelled basal bodies.

55  
56  
57  
58 141 The relative position of YFP::*TbFOR20* on mature basal bodies (Fig. 1B) was  
59 142 determined by dual fluorescence experiments with monoclonal antibody YL1/2, which  
60 143 recognises the C-terminal 'D-D-F' and 'E-E-Y' epitopes of mature basal body localised

144 *TbRP2* and/or tyrosinated  $\alpha$ -tubulin, respectively (André et al. 2014, Wehland et al. 1984).  
145 Here we performed immunofluorescence analysis of detergent extracted cytoskeletons (Fig.  
146 1B) and isolated flagella (Fig. 2). On cytoskeletal images there was ambiguity as to whether  
147 YL1/2 lay distal, proximal or coincident with YFP::*TbFOR20*. Detergent and NaCl extraction  
148 of *T. brucei* cells yields axonemes plus associated paraflagellar rod, transition zone  
149 microtubules, and basal bodies. Analysis of flagella isolated by detergent and then NaCl  
150 extraction revealed spatial separation of YL1/2 immunofluorescence and YFP::*TbFOR20*  
151 signals, with the former lying proximal to YFP::*TbFOR20* (Fig. 2A). In our earlier work (André  
152 et al. 2014) we proposed that at mature trypanosome basal bodies *TbRP2* is an antigen  
153 recognised by YL1/2. Given the spatial resolution of YL1/2 immunofluorescence and  
154 YFP::*TbFOR20* signals we were able to further question the identity of the trypanosome  
155 antigen(s) recognised by YL1/2. Indirect immunofluorescence of isolated flagella using a  
156 specific anti-*TbRP2* antibody (André et al. 2014) revealed that on mature basal bodies  
157 *TbRP2* is also proximal to YFP::*TbFOR20* (Fig. 2D), consistent with the idea that YL1/2  
158 recognises *TbRP2* rather than tyrosinated  $\alpha$ -tubulin. The final piece of experimental  
159 evidence that YL1/2 indeed specifically recognises *TbRP2* as its basal body antigen is the  
160 observation that YL1/2 detects by immunoblot not merely recombinant *TbRP2* (as we  
161 reported previously, André et al. 2014,) but also native *TbRP2* from trypanosome extracts  
162 (Fig. 3). We return to this point in the discussion.

163 Analysis of cells from early stages of the cell division cycle, when maturation of the  
164 probasal body assembled in the previous cell cycle occurs and elongation of the new  
165 flagellum begins, indicated duplication of YFP::*TbFOR20* fluorescence signals was  
166 coincident with new probasal body biogenesis and kinetoplast replication (Fig. 1C).  
167 Localisation of YFP::*TbFOR20* to both pro- and mature basal bodies was then retained  
168 throughout the remainder of the cell cycle (data not shown). In terms of length and motif  
169 architecture full length *TbFOR20* closely resembles a C-terminal truncated variant of *TbRP2*,  
170 *TbRP2*<sup>A134-463</sup>::myc, which localises only to mature basal bodies in *T. brucei* (André et al.  
171 2014). To confirm pro- and mature basal body localisations for YFP::*TbFOR20* was not an  
172 artefact of the N-terminal YFP tag, we also expressed in *T. brucei* *TbFOR20* with a C-  
173 terminal myc-epitope (*TbFOR20*::myc). Again, tagged protein was targeted to both pro- and  
174 mature basal bodies (Fig. 1D). Moreover, on isolated flagella *TbFOR20*::myc, as with  
175 YFP::*TbFOR20*, lies distal to *TbRP2* (Fig. 2E). Collectively, our localisation data indicate  
176 neither the nature nor the position of the tag influence protein localisation.

## 177 An N-terminal extension particular to FOR20 from African trypanosome species

179 We looked for differences between *TbFOR20*, *TbRP2*, and the other two trypanosome  
180 proteins with coupled TOF-LisH motifs (*TbOFD1*, *TbFOP/FOP1*-like, which are both mature  
181 basal body proteins; Fig. 2B-C) that could offer insight into why only *TbFOR20* is additionally  
182 targeted to probasal bodies, we noted (i) the distance from start methionine to the TOF motif  
183 is approximately twenty amino acids longer in the protein encoded by the *TbFOR20* gene  
184 model and (ii) this short N-terminal extension, enriched for negatively charged amino acids,  
185 appeared to be unique to mammal-infective African trypanosome species. Thus, the start  
186 methionine for FOR20 orthologues from a taxonomically diverse range of flagellate  
187 eukaryotes, a free-living trypanosomatid relative, *Bodo saltans*, and for other  
188 trypanosomatids, including the American trypanosome species *T. cruzi* and *T. rangeli*, plus  
189 their phylogenetically close relation *T. grayi*<sup>1</sup> (Kelly et al. 2014), and different *Leishmania*  
190 species all lie immediately upstream of the TOF motif (Fig. 4). We checked whether in the  
191 gene models predicted for FOR20 from *T. cruzi* and *L. major* (where, along with *T. brucei*,  
192 genome assembly and annotation is possibly the most exhaustive) the start codon could

<sup>1</sup> Although *T. grayi* is a parasite of African crocodiles.

193 have been called incorrectly, and that the open reading frame therefore extended upstream  
1 194 to an alternative start codon. We found no evidence to suggest that this was the case.  
2 195 Moreover, a near absence of introns in trypanosomatid genomes means examples of *cis*-  
3 196 splicing are extremely rare. Thus, we believe the start codons predicted for FOR20  
4 197 orthologues from *T. cruzi* and *Leishmania*, and by inference other trypanosomatids, are  
5 198 correct.

7 199 In *TbFOR20*, we also noted a methionine immediately upstream of the TOF motif that  
8 200 could conceivably provide the start codon for a shorter protein, although this downstream  
9 201 methionine is not present in the syntenic orthologues from two other African trypanosome  
10 202 species, *T. congolense* and *T. vivax*, for which nuclear genome sequences are available.  
11 203 Nonetheless, to confirm the authenticity of the predicted start codon for *TbFOR20* we  
12 204 compared the localisation of C-terminally myc-tagged *TbFOR20* variant translated from the  
13 205 downstream methionine (*TbFOR20*<sup>Δ1-21</sup>::myc) with the localisations of full length  
14 206 *TbFOR20*::myc and YFP::*TbFOR20* (in which YFP was fused in frame with the upstream  
15 207 methionine). Despite expression from a strong, doxycycline-inducible procyclin transcription  
16 208 promoter, *TbFOR20*<sup>Δ1-21</sup>::myc did not localise to pro- or mature basal bodies, but instead  
17 209 accumulated throughout the cell body (Fig. 5A). Thus, the short N-terminal extension unique  
18 210 to FOR20 from mammal-infective African trypanosome species is essential for basal body  
19 211 targeting, and moreover its role in basal body targeting is not masked by fusion of *TbFOR20*  
20 212 at its N-terminus to YFP.

24 213 To query the possible structural conformation adopted by the N-terminal extension,  
25 214 we submitted *TbFOR20* to analysis at the Phyre<sup>2</sup> web portal (Kelley et al. 2015). The α-  
26 215 helical conformations of the TOF and LisH motifs were accurately predicted and an equally  
27 216 confident prediction of disorder was noted for the short trypanosome FOR20 N-terminal  
28 217 extension (Fig. 6). Limited site directed mutagenesis within TOF and LisH motifs of  
29 218 *TbFOR20* revealed that both motifs were required for efficient basal body targeting. Three  
30 219 site-directed mutants were examined (E37A, F54A, Y88A; Fig. 7): for the E37A mutation  
31 220 overall protein expression levels were lower than for the other two site-directed mutants  
32 221 (Supp. Fig. 1B) and basal body targeting was completely abrogated (Fig. 7A). For F54A and  
33 222 Y88A mutations, where steady state accumulation of protein was much higher than for the  
34 223 E37A mutation, some protein was present at the basal/probasal body region (Fig. 7B-C) in  
35 224 detergent-extracted cytoskeletons although the localisation did not replicate the basal  
36 225 body/probasal body localisation seen for both YFP::*TbFOR20* and *TbFOR20*::myc (Fig. 1) in  
37 226 that the typical two-dot basal/probasal body *TbFOR20* signals were not seen. Instead a  
38 227 single focus or sometimes multiple foci of *TbFOR20* fluorescence was observed; where a  
39 228 single *TbFOR20* signal was seen this was often offset from the mature basal body signal of  
40 229 *TbRP2*. The images shown in Fig. 7 were captured using identical acquisition parameters.  
41 230 Since F54A and Y88A mutant proteins readily accumulated in the cytoplasm of intact cells  
42 231 the representative localisation data (Fig.7B-C) is also suggestive of inefficient protein  
43 232 targeting to pro- and mature basal bodies.

#### 233 234 *TbFOR20* N-terminal extension is insufficient to re-target *TbRP2*<sup>Δ134-463</sup>::myc

235 To investigate further the possible role of the extension in *TbFOR20* and the orthologues  
236 from African trypanosome species closely related to *T. brucei*, we determined whether the  
237 addition of the N-terminal 21 amino acids from *TbFOR20* to amino acids 2-133 of *TbRP2*  
238 would be sufficient to direct the protein chimera *TbFOR20*<sup>Δ22-151</sup>::*RP2*<sup>Δ1/Δ134-463</sup>::myc to both  
239 pro- and mature basal bodies in *T. brucei* – since *TbRP2*<sup>Δ134-463</sup>::myc closely resembles  
240 *TbFOR20* in length and motif architecture and incorporates efficiently into mature basal  
241 bodies (André et al. 2014). Despite efficient expression of protein, localisation to mature  
242 basal bodies only, was observed throughout the cell division cycle (*i.e.* at the start of the cell

243 cycle when cells possess one flagellum, one probasal body, one nucleus and one  
1 244 kinetoplast (1K1N); following kinetoplast replication but pre-mitosis when cells possess two  
2 245 flagella, two probasal bodies and one nucleus (2K1N); and post-mitosis (2K2N)) (Fig. 5B).

3  
4 246  
5  
6 247 Heterologously expressed *T. cruzi* FOR20 (with no extension) localises to pro- and  
7  
8 248 mature basal bodies in *T. brucei*

9  
10 249 In a final set of targeting experiments we asked where in a *T. brucei* cell would a  
11 250 trypanosomatid FOR20 in which an N-terminal extension is not normally present be found  
12 251 when expressed heterologously. For this analysis we amplified by PCR the FOR20 open-  
13 252 reading frame from *T. cruzi* (Sylvio X10 strain) and cloned the resulting amplicon into HindIII-  
14 253 XhoI-digested expression plasmid pDEX377<sub>TbRP2::myc</sub> such that *Tc*FOR20 would be  
15 254 expressed with a C-terminal myc-epitope tag in *T. brucei*. Dual immunofluorescence studies  
16 255 with either BBA4 (Fig. 5C) or affinity-purified anti-*Tb*RP2 antibodies (Fig. 5D) indicated that  
17 256 despite the absence of the N-terminal extension seen in *Tb*FOR20, *Tc*FOR20 is readily  
18 257 incorporated into pro- and mature basal bodies. The images shown in Fig. 5C-D are of  
19 258 detergent-extracted cytoskeletons, thereby confirming the stable incorporation of *Tc*FOR20  
20 259 into *T. brucei* basal bodies.

## 23 260

## 25 261 Discussion

27 262 In a wider evolutionary context trypanosomatids and their free-living kinetoplastid relatives  
28 263 belong to the eukaryotic super group Excavata. Widely accepted as evolutionarily divergent  
29 264 unicellular eukaryotes (Akiyoshi and Gull 2013, Hampl et al. 2009, Katz and Grant 2015,  
30 265 Rogozin et al. 2009), cell shape and morphogenesis in these organisms is defined by a  
31 266 microtubule-based cytoskeleton. Extensive cytoskeletal remodelling and major alterations in  
32 267 cell morphology are observed during generally complex trypanosomatid life cycles (Sharma  
33 268 et al. 2008, Peacock et al. 2014) although changes in expression of just a single regulatory  
34 269 protein can control the developmental pattern of morphogenesis undertaken by *T. brucei* in  
35 270 its tsetse fly vector (Kolev et al. 2012). Gene duplication events and variations in the  
36 271 abundance of some individual cytoskeletal proteins also provide stage-specific regulation or  
37 272 life stage-relevant influences on trypanosome morphology (Hayes et al. 2014, Olego-  
38 273 Fernandez et al. 2009, Portman and Gull 2014, Sunter et al. 2015, Vedrenne et al. 2002).  
39 274 Differences between trypanosomatids with respect to domain or motif architectures in a few,  
40 275 lineage-specific cytoskeletal proteins have also been reported (e.g. Vaughan et al. 2008).  
41 276 Identification of a curious N-terminal extension in FOR20 orthologues from mammal-infective  
42 277 African trypanosomes not evident in any other eukaryote and enriched in acidic amino acids,  
43 278 adds a further molecular variation to our understanding of the sculpture and evolution of  
44 279 trypanosomatid cytoskeletons. Yet, trypanosomatids also provide tractable models for  
45 280 studying cytoskeletal processes conserved widely in eukaryotic evolution. Flagellum  
46 281 assembly, structure and function provide prime examples of where trypanosomes provide a  
47 282 useful model system for interrogating conserved gene function (Broadhead et al. 2006,  
48 283 Vincensini et al. 2011).

## 53 284

## 55 285 Probing FOR20 function and localisation

57 286 FOR20 localisation and function was previously studied in the ciliate *Paramecium*  
58 287 *tetraurelia* (Bengueddach et al. 2017, Aubusson-Fleury et al. 2012). Differences in basal  
59 288 body assembly and maturation processes between *T. brucei* and *P. tetraurelia* are

289 potentially informative in questioning FOR20 function. In both *Paramecium* and  
1 290 trypanosomatids, a non-ciliated basal body is physically associated with a mature basal body  
2 291 from which an axoneme is extended. In ciliates, the basal body transition zone is present  
3 292 and docked at the plasma membrane, irrespective of whether the basal body is ciliated or  
4 293 not (Aubusson-Fleury et al. 2012, Tassin et al. 2015). FOR20 is present at or immediately  
5 294 above the terminal plate (the most proximal boundary) of the ciliate transition zone of both  
6 295 ciliated and non-ciliated *Paramecium* basal bodies (Aubusson-Fleury et al. 2012). The distal  
7 296 region of the transition zone in non-ciliated basal bodies is subject to re-modelling coincident  
8 297 with the start of axoneme elongation (Aubusson-Fleury et al. 2012, Tassin et al. 2015). In  
9 298 contrast, *T. brucei* probasal bodies form orthogonal to their associated mature basal body.  
10 299 New probasal bodies form early in the cell cycle, coincident with maturation of the probasal  
11 300 body formed in the previous cell cycle, and re-orientate from orthogonal to parallel with the  
12 301 associated mature basal body prior to mitosis (~0.4 of a cell cycle later). Even when  
13 302 reoriented there is clearly a region of cytosol between the distal end of the probasal body  
14 303 and the flagellar pocket membrane (e.g. Höög et al. 2014, Lacomble et al. 2009). Following  
15 304 reorientation, the transition zone forms in the next cell cycle, as doublet microtubules extend  
16 305 from the triplet microtubule barrel (Vaughan and Gull 2015). Transition zone extension is  
17 306 accompanied by transitional fibre formation, membrane docking and continues with  
18 307 elongation of the axoneme proper (Lacomble et al. 2010, Woodward et al. 1995). In our  
19 308 view, early recruitment of *TbFOR20* to the distal end of orthogonal trypanosome probasal  
20 309 bodies and the distance between the re-orientated probasal bodies and the plasma  
21 310 membrane argue against a direct role for little-understood FOR20 in basal body-membrane  
22 311 docking, or at least that a role for FOR20 in docking is not conserved in all flagellate  
23 312 eukaryotes. We also note there is no evidence of motifs or domains associated with protein-  
24 313 lipid/membrane interaction seen in FOR20 proteins.

28  
29 314 Additional to studying *TbFOR20* localisation, we also subjected *TbFOR20* to gene-  
30 315 specific RNAi. Despite ~90% reduction in YFP::*TbFOR20* detectable by immunoblot (Supp.  
31 316 Fig. 1E), no morphology phenotype was discernible over the course of six successive cell  
32 317 cycles - normally ample enough time for phenotypes to develop following RNAi against  
33 318 essential flagellum or basal body components. Failure to observe any RNAi phenotype may  
34 319 indicate that the small amount of FOR20 still produced is sufficient for normal cell function, a  
35 320 critical importance for *TbFOR20* only in other life cycle stages – our experiments were all  
36 321 performed with cultured procyclic trypomastigotes, which normally replicate within a tsetse  
37 322 fly midgut – or functional redundancy. We note that a previous genome-wide survey of gene  
38 323 function also failed to elicit a *TbFOR20* RNAi phenotype in either procyclic or pathogenic  
39 324 bloodstream form *T. brucei* (Alsford et al. 2011). Further clues to the role(s) of FOR20 in  
40 325 flagellum assembly or function, however, perhaps comes from the localisation of FOR20 in  
41 326 *Giardia intestinalis*, another excavate protist. Here, hemagglutinin-tagged *Giardia* FOR20  
42 327 localises along the length of paraflagellar dense rods associated with the cytoplasmic  
43 328 regions of axonemes that form anterior, posterior-lateral and immotile caudal flagella  
44 329 (Lauwaet et al. 2011). Using transmission electron microscopy, Hoeng et al. (2008)  
45 330 demonstrated the cytoplasmic regions of *Giardia* axonemes, which run for a considerable  
46 331 distance through the cytoplasm before exit from the cell body, do not correspond to  
47 332 elongated transition zones, but instead exhibit conventional '9+2' architecture. Thus,  
48 333 localisation of FOR20 orthologues in both *T. brucei* and *G. intestinalis* are not consistent with  
49 334 conservation of a direct role for FOR20 in basal body-membrane docking. Given its small  
50 335 size and paucity of recognisable domain architecture (other than TOF-LisH motifs, which  
51 336 assume  $\alpha$ -helical secondary structure and mediate protein oligomerisation (Mikolajka et al.  
52 337 2006, Sedjai et al. 2010)), it appears unlikely that FOR20 exhibits any intrinsic enzymatic  
53 338 activity. FOR20 also stands alone among FOP family proteins in that the protein lacks  
54 339 extensive amino acid sequence and domain architecture downstream of N-terminal TOF-  
55 340 LisH-PLL motifs. Conceivably, FOR20 acts as an adapter or linking protein for scaffolding  
56 341 and/or stabilisation of other proteins or complexes for flagellum assembly and/or basal body



342 docking, albeit that protein function appears non-essential in procyclic *T. brucei* under  
1 343 standard culture conditions.

## 3 344 4 5 345 On the antigen specificity of YL1/2 at the *T. brucei* basal body

7 346 Our ongoing interests in characterising the functions of trypanosome FOP family proteins  
8 347 has seen us question the identity of the basal body antigen recognised by the monoclonal  
9 348 antibody YL1/2. For over 30 years, YL1/2 has been used as a marker for tyrosinated  $\alpha$ -  
10 349 tubulin in eukaryotic cells (Kilmartin et al. 1982). In trypanosomatids, YL1/2 has been used  
11 350 widely in studies defining critical events in cell morphogenesis and division (e.g. Sherwin et  
12 351 al. 1987, Wheeler et al. 2013). With cell shape so heavily dependent on a sub-pellicular  
13 352 microtubule corset remodelled and inherited in a semi-conservative manner (Sherwin and  
14 353 Gull 1989), YL1/2 is perfect for marking growth of new microtubules in which the C-terminal  
15 354 epitope of  $\alpha$ -tubulin is recognisable prior to detyrosination. Yet, the prominent mature basal  
16 355 body signal observed in YL1/2 immunofluorescence of trypanosomatids presents a  
17 356 conundrum in that the centriole barrel is composed of mature microtubules and other anti-  
18 357 tubulin antibodies do not yield an immunofluorescence focus comparable to the YL1/2 basal  
19 358 body signal. It was proposed that this YL1/2 basal body signal represents a dynamic pool of  
20 359 tyrosinated  $\alpha$ -tubulin awaiting IFT-mediated transport to the flagellar distal tip (Stephan et al.  
21 360 2007). In that regard, we note that the axoneme of new, elongating flagella in trypanosomes  
22 361 is also readily detected using YL1/2 (Sherwin et al. 1987). With our demonstration that YL1/2  
23 362 readily detects by immunoblot both recombinant TbRP2 (André et al. 2014) and native  
24 363 TbRP2 (this study), the notion that basal body localised YL1/2 detects tyrosinated  $\alpha$ -tubulin  
25 364 must be called into question. Note we do not call into question the value of using YL1/2 to  
26 365 detect tyrosinated  $\alpha$ -tubulin at other cellular locations in trypanosomatids. The caution that  
27 366 we encourage echoes caveats offered by Wehland and colleagues when they mapped the  
28 367 epitope specificity of YL1/2 in their seminal study (Wehland et al. 1984).

32  
33 368 In questioning where along the length of pro- and mature basal bodies *TbFOR20* is  
34 369 found, we have mapped the localisation of *TbFOR20*, *TbOFD1* and *TbFOP/FOP1*-like  
35 370 proteins relative to basal body antigen recognised by YL1/2, which we believe is the fourth  
36 371 trypanosome FOP family protein *TbRP2*. Although one considers the transitional fibres  
37 372 where *TbRP2* is found to be at the junction of the triplet to doublet microtubule basal body  
38 373 transition and attach to the base of the flagellar pocket membrane contributing to a physical  
39 374 ciliary gate (Garcia-Gonzalo FR and Reiter JF 2017), our immunofluorescence analysis of  
40 375 isolated flagella indicates *TbRP2* proximal to *TbFOR20* with no evidence of *TbFOR20* re-  
41 376 localisation concomitant with transition zone elongation during pro- to basal body maturation.  
42 377 Returning to the original immunogold localisation of YL1/2 in *T. brucei* (Stephan et al. 2007)  
43 378 it is clear that there is extensive gold labelling at the level of the triplet microtubule barrel,  
44 379 consistent with the immunolocalisation data presented here. Collectively, relative  
45 380 localisations of the complete trypanosome FOP protein family can be summarised by the  
46 381 model shown in Fig. 8. The model highlights subtle, yet realistically functionally significant  
47 382 differences in the basal body localisations of trypanosome FOP family proteins. Future  
48 383 studies are likely to provide insight into whether these localisation differences are more  
49 384 broadly conserved and how they might relate to functional specialisation.

## 53 385 54 55 386 Subtleties in TOF-LisH motif-dependent targeting of centriolar proteins

57 387 The prediction of a short N-terminal extension for FOR20 orthologues from mammal-  
58 388 infective African *Trypanosoma* species was intriguing, not least because it is among  
59 389 *Leishmania* species where the average length of orthologous coding sequences is predicted

390 to be larger by ~15-20% than in other trypanosomatids (El-Sayed et al. 2005). Following  
1 391 initial annotations of the *T. brucei* nuclear genome, RNAseq analyses saw identification of an  
2 392 essential 'small proteome' and re-annotation of many trypanosome protein-coding genes,  
3 393 revealing alternative sites for *trans*-splicing (the mechanism by which the 5'-end of all  
4 394 protein-coding transcripts are capped) and the use of alternative start codons (Ericson et al.  
5 395 2014, Kolev et al. 2010, Nilsson et al. 2010, Siegel et al. 2010). Thus, it was necessary to  
6 396 confirm the presence of a candidate N-terminal extension in *TbFOR20* and exclude the use  
7 397 of a potential downstream start methionine. Our analyses revealed that the extension is  
8 398 essential for localisation of *TbFOR20* at pro- and mature basal bodies, but its function in  
9 399 ensuring protein targeting is not masked by the presence of a large (~28 kDa), globular N-  
10 400 terminal YFP tag.

13 401 The TOF-LisH motif combination is a conserved, if seldom used, feature of centriolar  
14 402 proteins. In mammalian cells inappropriate use of TOF-LisH targeting can have pathological  
15 403 consequences (Lelièvre et al. 2008). Thus, there is wider interest in understanding how  
16 404 TOF-LisH motif combinations mediate centriolar localisation. The cryptic nature of how the  
17 405 *TbFOR20* N-terminal extension contributes to pro- and mature basal body targeting,  
18 406 combined with the observation that *TcFOR20*, which naturally lacks any N-terminal  
19 407 extension, readily localises to *T. brucei* pro- and mature basal bodies indicate there remains  
20 408 much to learn regarding how TOF-LisH motif combinations, and additional motif elements,  
21 409 contribute to the targeting of different proteins to distinct basal body sites. Successive C-  
22 410 terminal deletions of *TbRP2* all target myc-epitope tagged proteins to mature trypanosome  
23 411 basal bodies providing the TOF-LisH motifs remain intact (André et al. 2014). This suggests  
24 412 a principal functional role of these motifs is to confer protein targeting. RNAi phenotypes of  
25 413 *T. brucei* FOP family proteins show no discernible overlap, and proteomic screening has not  
26 414 identified any other FOP family member as an interacting or near neighbour protein to  
27 415 *TbRP2*<sup>2</sup>. These observations emphasise a likely importance of molecule-specific interactions  
28 416 in underpinning the use of this efficient targeting determinant to eukaryotic basal bodies.

## 32 417 33 34 418 **Methods**

36 419 **Cell culture:** Procyclic *T. brucei* (cell line 927smox; Poon et al. 2012; Lister strain 427) were cultured  
37 420 in SDM-79 medium containing 10% v/v heat-inactivated foetal bovine serum, as described previously  
38 421 (Brun and Schönberger, 1979). Constitutive expression of YFP- and myc epitope-tagged proteins  
39 422 occurred in a 427 genetic background. *TbFOR20::myc* proteins (full length and without the N-terminal  
40 423 extension) were also expressed in a 927smox background. 927smox is genetically modified to  
41 424 express a tetracycline-repressor protein and T7 RNA polymerase, meaning these cells are amenable  
42 425 to inducible gene expression or RNAi. The *TbRP2* RNAi mutant (on a 927smox background) was  
43 426 generated as described previously (André et al. 2014). *TbFOR20* RNAi was also induced on a  
44 427 927smox background. *TbFOR20*<sup>Δ22-151::RP2<sup>Δ1/Δ134-463</sup>::myc</sup> (sub-cloned as described below) and  
45 428 *TcFOR20::myc* were constitutively expressed in a 427 background. Cells were transfected and stable  
46 429 transformants selected using blasticidin (10 μg ml<sup>-1</sup>) or hygromycin B (50 μg ml<sup>-1</sup>) according to  
47 430 standard methods (McCulloch et al. 2004).

49  
50 431 **Plasmid constructs:** For constitutive expression of YFP-tagged *TbFOR20* and *TbOFD1* (André et al.  
51 432 2016) from endogenous chromosomal loci amplicons corresponding to XbaI-XhoI digested partial  
52 433 open reading frames and XhoI-BamHI-digested upstream intergenic regions were sub-cloned in  
53 434 three-way ligations into XbaI-BamHI-digested pEnT6B-Y (Kelly et al. 2007). For expression of myc  
54 435 epitope-tagged *TbFOR20* variants and *TcFOR20*, open reading frames minus the stop codon were  
55 436 PCR amplified using forward and reverse priming oligonucleotides synthesised with HindIII and XhoI  
56 437 restriction sites at the 5' end, respectively. HindIII-XhoI-digested PCR amplicons were then ligated  
57 438 with HindIII-XhoI-digested pDEX377<sub>TbRP2::myc</sub> (André et al. 2014). To prepare a chimeric gene for  
58 439 expression of the first 21 amino acids of *TbFOR20* fused to amino acids 2-133 of *TbRP2* a two-step

60 <sup>2</sup> Qi X et al. in preparation.  
61  
62  
63  
64  
65

440 PCR strategy was used. Using gDNA template, forward primer 5'-  
1 441 ggcgagagtcctttaacgcacccgaggcgactacaacctaccaagcgaagg-3' and reverse primer  
2 442 5'ttaggatccgctattggcaccgccgcccgggtg-3' (BamHI site italicised) was used to amplify coding  
3 443 sequence for amino acids 2-133 of *TbRP2* preceded in frame by amino acids 11-21 of *TbFOR20*. The  
4 444 resulting PCR amplicon was purified and used as template for a second PCR using the same reverse  
5 445 primer as PCR 1, but with a new forward primer, 5'-  
6 446 cgcaagcctatggaggaaagggaggaggaggtgaggcgagagtcctttaacgc (HindIII site underlined), to create  
7 447 coding sequence with the amino acids 1-10 from *TbFOR20* also added. The resulting purified PCR  
8 448 amplicon was digested with BamHI and HindIII and ligated with HindIII-XhoI-digested  
9 449 pDEX377<sub>TbRP2::myc</sub>, thereby creating pDEX377<sub>TbFOR20Δ22-151::RP2Δ1/Δ134-463::myc</sub>. For *TbFOR20* RNAi the  
10 450 open reading frame was sub-cloned into BamHI-HindIII-digested p2T7<sub>177</sub> (Wickstead et al. 2002).  
11 451 NotI-digested constructs with genes encoding C-terminal myc-tagged proteins or *TbFOR20* RNAi  
12 452 insert were transfected as described above. All plasmids were sequenced using ABI prism  
13 453 sequencing technology (Source Bioscience).

15 454 **Microscopy and immunoblotting:** For fluorescence microscopy, cells were settled onto glass  
16 455 coverslips and either fixed directly with paraformaldehyde (3.7 % w/v in PBS) or extracted for 0.5 min  
17 456 with PEME containing 1% v/v NP-40 prior to fixation. For preparation of isolated flagella, exponentially  
18 457 growing cells were harvested and cytoskeletons extracted on ice for 10 minutes in PEME 1% v/v NP-  
19 458 40. Cytoskeleton pellets were harvested and flagella extracted twice on ice for 10 minutes in PEME  
20 459 1M NaCl; flagella were collected by centrifugation after each extraction (13000 g, 30 min, 4°C), before  
21 460 settling onto glass coverslips. Fixed preparations were decorated for indirect immunofluorescence  
22 461 with the monoclonal antibodies BBA4 or YL1/2 as described previously (Woodward et al. 1995 and  
23 462 Sherwin et al. 1987, respectively) and decoration with the anti-myc monoclonal antibody was  
24 463 performed following the instructions of the supplier (Myc, Abcam). Cells were imaged at 60x  
25 464 magnification using either an Applied Precision DeltaVision Microscope and a Roper Scientific  
26 465 Photometrics Cool SNAP HQ camera or for the images shown in Fig. 2D-E a LSM880 Laser  
27 466 Scanning Confocal microscope (Zeiss). Expected sizes of all tagged proteins expressed in the study  
28 467 were confirmed by immunoblotting (Supp. Fig. 1); 10% acrylamide gels were used for SDS-PAGE  
29 468 prior to protein transfer onto Hybond P membranes (GE Healthcare).

## 470 Acknowledgements

36 471 This work was in part supported by grants BBG0210581 andBBF0109311 awarded to MLG  
37 472 and PGM by the UK Biological and Biotechnological Sciences Research Council. We thank  
38 473 Kevin Tyler (UEA, UK) for the kind gift of *T. cruzi* genomic DNA.

## 475 References

44 476 **Absalon S, Blisnick T, Kohl L, Toutirais G, Dore G, Julkowska D, Tavenet A, Bastin P**  
45 477 (2008) Intraflagellar transport and functional analysis of genes required for flagellum  
46 478 formation in trypanosomes. *Mol Biol Cell* 19:929-944.

48 479 **Akiyoshi B, Gull K** (2013) Evolutionary cell biology of chromosome segregation: insights  
49 480 from trypanosomes. *Open Biol* 3:130023.

51 481 **Alsford S, Turner DJ, Obado SO, Sanchez-Flores A, Glover L, Berriman M, Hertz-**  
52 482 **Fowler C, Horn D** (2011) High-throughput phenotyping using parallel sequencing of RNA  
53 483 interference targets in the African trypanosome. *Genome Res* 21:915-924.

55 484 **André J, Harrison S, Towers K, Qi X, Vaughan S, McKean PG, Ginger ML** (2013) The  
56 485 tubulin cofactor C family member TBCCD1 orchestrates cytoskeletal filament formation. *J*  
57 486 *Cell Sci* 126:5350-5356.

487 **André J, Kerry L, Qi X, Hawkins E, Drizyte K, Ginger ML, McKean PG** (2014) An  
1 488 alternative model for the role of RP2 protein in flagellum assembly in the African  
2 489 trypanosome. *J Biol Chem* 289:464-475.  
3  
4 490 **Aubusson-Fleury A, Lemullois M, de Loubresse NG, Laligne C, Cohen J, Rosnet O,**  
5 491 **Jerka-Dziadosz M, Beisson J, Koll F** (2012) The conserved centrosomal protein FOR20 is  
6 492 required for assembly of the transition zone and basal body docking at the cell surface. *J*  
7 493 *Cell Sci* 125:4395-4404.  
8  
9 494 **Azimzadeh J, Nacry P, Christodoulidou A, Drevensek S, Camilleri C, Amiour N, Parcy**  
10 495 **F, Pastuglia M, Bouchez D** (2008) *Arabidopsis* TONNEAU1 proteins are essential for  
11 496 preprophase band formation and interact with centrin. *Plant Cell* 20:2146-2159.  
12  
13 497 **Bengueddach H, Lemullois M, Aubusson-Fleury A, Koll F** (2017) Basal body positioning  
14 498 and anchoring in the multiciliated cell *Paramecium tetraurelia*: roles of OFD1 and VFL3. *Cilia*  
15 499 6:6.  
16  
17 500 **Broadhead R, et al.** (2006) Flagellar motility is required for the viability of the bloodstream  
18 501 trypanosome. *Nature* 440:224-227.  
19  
20 502 **Brun R, Schönenberger M** (1979) Cultivation and in vitro cloning or procyclic culture forms  
21 503 of *Trypanosoma brucei* in a semi-defined medium. Short communication. *Acta Trop* 36: 289-  
22 504 292.  
23  
24 505 **Carvalho-Santos Z, Azimzadeh J, Pereira-Leal JB, Bettencourt-Dias M** (2011) Evolution:  
25 506 Tracing the origins of centrioles, cilia, and flagella. *J Cell Biol* 194:165-175.  
26  
27 507 **Davidge JA, Chambers E, Dickinson HA, Towers K, Ginger ML, McKean PG, Gull K**  
28 508 (2006) Trypanosome IFT mutants provide insight into the motor location for mobility of the  
29 509 flagella connector and flagellar membrane formation. *J Cell Sci* 119:3935-3943.  
30  
31 510 **Dawe HR, Farr H, Gull K** (2007) Centriole/basal body morphogenesis and migration during  
32 511 ciliogenesis in animal cells. *J Cell Sci* 120:7-15.  
33  
34 512 **El-Sayed NM, et al.** (2005) Comparative genomics of trypanosomatid parasitic protozoa.  
35 513 *Science* 309:404-409.  
36  
37 514 **Ericson M, Janes MA, Butter F, Mann M, Ullu E, Tschudi C** (2014) On the extent and role  
38 515 of the small proteome in the parasitic eukaryote *Trypanosoma brucei*. *BMC Biol* 12:14.  
39  
40 516 **Fritz-Laylin LK, Cande WZ** (2010) Ancestral centriole and flagella proteins identified by  
41 517 analysis of *Naegleria* differentiation. *J Cell Sci* 123:4024-4031.  
42  
43 518 **Fritz-Laylin LK, Levy YY, Levitan E, Chen S, Cande WZ, Lai EY, Fulton C** (2016) Rapid  
44 519 centriole assembly in *Naegleria* reveals conserved roles for both de novo and mentored  
45 520 assembly. *Cytoskeleton (Hoboken)* 73:109-116.  
46  
47 521 **Garcia-Gonzalo FR, Reiter JF** (2017) Open Sesame: how transition fibres and the  
48 522 transition zone control ciliary composition. *Cold Spring Harb Perspect Biol* 9:a028134.  
49  
50 523 **Gleunz E, Povelones ML, Englund PT, Gull K** (2011) The kinetoplast duplication cycle in  
51 524 *Trypanosoma brucei* is orchestrated by cytoskeleton-mediated cell morphogenesis. *Mol Cell*  
52 525 *Biol* 31:1012-1021.  
53  
54 526 **HAMPL V, Hug L, Leigh JW, Dacks JB, Lang BF, Simpson AG, Roger AJ** (2009)  
55 527 Phylogenomic analyses support the monophyly of Excavata and resolve relationships  
56 528 among eukaryotic "supergroups". *Proc Natl Acad Sci U S A* 106:3859-3864.  
57  
58 529 **Hayes P, Varga V, Olego-Fernandez S, Sunter J, Ginger ML, Gull K** (2014) Modulation of  
59 530 a cytoskeletal calpain-like protein induces major transitions in trypanosome morphology. *J*  
60 531 *Cell Biol* 206:377-384.  
61  
62 532 **Hodges ME, Scheumann N, Wickstead B, Langdale JA, Gull K** (2010) Reconstructing the  
63 533 evolutionary history of the centriole from protein components. *J Cell Sci* 123:1407-1413.  
64  
65

534 **Hoeng JC, Dawson SC, House SA, Sagolla MS, Pham JK, Mancuso JJ, Lowe J, Cande**  
1 535 **WZ** (2008) High-resolution crystal structure and in vivo function of a kinesin-2 homologue in  
2 536 *Giardia intestinalis*. Mol Biol Cell 19:3124-3137.  
3  
4 537 **Höög JL, Lacomble S, O'Toole ET, Hoenger A, McIntosh JR, Gull K** (2014) Modes of  
5 538 flagellar assembly in *Chlamydomonas reinhardtii* and *Trypanosoma brucei*. ELife 3:e01479.  
6  
7 539 **Katz LA, Grant JR** (2015) Taxon-rich phylogenomic analyses resolve the eukaryotic tree of  
8 540 life and reveal the power of subsampling by sites. Syst Biol 64:406-415.  
9  
10 541 **Keller LC, Romijn EP, Zamora I, Yates JR, 3rd, Marshall WF** (2005) Proteomic analysis of  
11 542 isolated *Chlamydomonas* centrioles reveals orthologs of ciliary-disease genes. Curr Biol  
12 543 15:1090-1098.  
13 544 **Kelley LA, Mezulis S, Yates CM, Wass MN, Sternberg MJE** (2015) The Phyre<sup>2</sup> webportal  
14 545 for protein modelling, prediction and analysis. Nat Protoc 10:845-858.  
15  
16 546 **Kelly S, Ivens A, Manna PT, Gibson W, Field MC** (2014) A draft genome for the African  
17 547 crocodilian trypanosome *Trypanosoma grayi*. Sci Data 1:140024.  
18  
19 548 **Kelly S, Reed J, Kramer S, Ellis L, Webb H, Sunter J, Salje J, Marinsek N, Gull K,**  
20 549 **Wickstead B, Carrington M** (2007) Functional genomics in *Trypanosoma brucei*: a  
21 550 collection of vectors for the expression of tagged protein from endogenous and ectopic gene  
22 551 loci. Mol Biochem Parasitol 154:103-109.  
23  
24 552 **Kilburn CL, Pearson CG, Romijn EP, Meehl JB, Giddings TH, Jr., Culver BP, Yates JR,**  
25 553 **3rd, Winey M** (2007) New *Tetrahymena* basal body protein components identify basal body  
26 554 domain structure. J Cell Biol 178:905-912.  
27  
28 555 **Kilmartin JV, Wright B, Milstein C** (1982) Rat monoclonal antitubulin antibodies derived by  
29 556 using a new nonsecreting rat cell line. J Cell Biol 93:576-582.  
30  
31 557 **Kolev NG, Ramey-Butler K, Cross GA, Ullu E, Tschudi C** (2012) Developmental  
32 558 progression to infectivity in *Trypanosoma brucei* triggered by an RNA-binding protein.  
33 559 Science 338:1352-1353.  
34  
35 560 **Kolev NG, Franklin JB, Carmi S, Shi H, Michaeli S, Tschudi C** (2010) The transcriptome  
36 561 of the human pathogen *Trypanosoma brucei* at single-nucleotide resolution. PLoS Pathog  
37 562 6:e1001090.  
38  
39 563 **Lacomble S, Vaughan S, Gadelha C, Morphew MK, Shaw MK, McIntosh JR, Gull K**  
40 564 (2010) Basal body movements orchestrate membrane organelle division and cell  
41 565 morphogenesis in *Trypanosoma brucei*. J Cell Sci 123:2884-2891.  
42  
43 566 **Lacomble S, Vaughan S, Gadelha C, Morphew MK, Shaw MK, McIntosh JR, Gull K**  
44 567 (2009) Three-dimensional cellular architecture of the flagellar pocket and associated  
45 568 cytoskeleton in trypanosomes revealed by electron microscope tomography. J Cell Sci  
46 569 122:1081-1090.  
47  
48 570 **Lauwaet T, Smith AJ, Reiner DS, Romijn EP, Wong CC, Davids BJ, Shah SA, Yates JR,**  
49 571 **3rd, Gillin FD** (2011) Mining the *Giardia* genome and proteome for conserved and unique  
50 572 basal body proteins. Int J Parasitol 41:1079-1092.  
51  
52 573 **Lee JY, Stearns T** (2013) FOP is a centriolar satellite protein involved in ciliogenesis. PLoS  
53 574 One 8:e58589.  
54  
55 575 **Lelièvre H, Chevrier V, Tassin AM, Birnbaum D** (2008) Myeloproliferative disorder FOP-  
56 576 FGFR1 fusion kinase recruits phosphoinositide-3 kinase and phospholipase C $\gamma$  at the  
57 577 centrosome. Mol Cancer 7:30.

578 **Mikolajka A, Yan X, Popowicz GM, Smialowski P, Nigg EA, Holak TA** (2006) Structure of  
1 579 the N-terminal domain of the FOP (FGFR1OP) protein and implications for its dimerization  
2 580 and centrosomal localization. *J Mol Biol* 359:863-875.

3  
4 581 **McCulloch R, Vassella E, Burton P, Boshart M, Barry JD** (2004) Transformation of  
5 582 monomorphic and pleomorphic *Trypanosoma brucei*. *Methods Mol Biol* 262: 53-86.

6 583 **Moran J, McKean PG, Ginger ML** (2014) Eukaryotic flagella: variations in form, function,  
7 584 and composition during evolution. *Bioscience* 64:1103-1114.

8  
9 585 **Nilsson D, Gunasekera K, Mani J, Osteras M, Farinelli L, Baerlocher L, Roditi I,**  
10 586 **Ochsenreiter T** (2010) Spliced leader trapping reveals widespread alternative splicing  
11 587 patterns in the highly dynamic transcriptome of *Trypanosoma brucei*. *PLoS Pathog*  
12 588 6:e1001037.

13  
14  
15 589 **Ogbadoyi EO, Robinson DR, Gull K** (2003) A high-order trans-membrane structural  
16 590 linkage is responsible for mitochondrial genome positioning and segregation by flagellar  
17 591 basal bodies in trypanosomes. *Mol Biol Cell* 14:1769-1779.

18  
19 592 **Olego-Fernandez S, Vaughan S, Shaw MK, Gull K, Ginger ML** (2009) Cell  
20 593 morphogenesis of *Trypanosoma brucei* requires the paralogous, differentially expressed  
21 594 calpain-related proteins CAP5.5 and CAP5.5V. *Protist* 160:576-590.

22  
23 595 **Peacock L, Bailey M, Carrington M, Gibson W** (2014) Meiosis and haploid gametes in the  
24 596 pathogen *Trypanosoma brucei*. *Curr Biol* 24:181-186.

25  
26 597 **Poon SK, Peacock L, Gibson W, Gull K, Kelly S** (2012) A modular and optimized single  
27 598 marker system for generating *Trypanosoma brucei* cell lines expressing T7 RNA polymerase  
28 599 and the tetracycline repressor. *Open Biol* 2:110037.

29  
30 600 **Portman N, Gull K** (2014) Identification of paralogous life-cycle stage specific cytoskeletal  
31 601 proteins in the parasite *Trypanosoma brucei*. *PLoS One* 9:e106777.

32  
33 602 **Prensier G, Dubremetz JF, Schrevel J** (2008) The unique adaptation of the life cycle of the  
34 603 coelomic gregarine *Diplauxis hatti* to its host *Perinereis cultrifera* (Annelida, Polychaeta): an  
35 604 experimental and ultrastructural study. *J Eukaryot Microbiol* 55:541-553.

36  
37 605 **Rogozin IB, Basu MK, Csuros M, Koonin EV** (2009) Analysis of rare genomic changes  
38 606 does not support the unikont-bikont phylogeny and suggests cyanobacterial symbiosis as  
39 607 the point of primary radiation of eukaryotes. *Genome Biol Evol* 1:99-113.

40  
41 608 **Sedjai F, et al.** (2010) Control of ciliogenesis by FOR20, a novel centrosome and  
42 609 pericentriolar satellite protein. *J Cell Sci* 123:2391-2401.

43  
44 610 **Sharma R, Peacock L, Gluenz E, Gull K, Gibson W, Carrington M** (2008) Asymmetric cell  
45 611 division as a route to reduction in cell length and change in cell morphology in  
46 612 trypanosomes. *Protist* 159:137-151.

47  
48 613 **Sherwin T, Schneider A, Sasse R, Seebeck T, Gull K** (1987) Distinct localisation and cell  
49 614 cycle dependence of COOH terminally tyrosinolated  $\alpha$ -tubulin in the microtubules of  
50 615 *Trypanosoma brucei brucei*. *J Cell Biol* 104:439-446.

51  
52 616 **Sherwin T, Gull K** (1989) Visualization of detyrosination along single microtubules reveals  
53 617 novel mechanisms of assembly during cytoskeletal duplication in trypanosomes. *Cell*  
54 618 57:211-221.

55  
56 619 **Siegel TN, Hekstra DR, Wang X, Dewell S, Cross GA** (2010) Genome-wide analysis of  
57 620 mRNA abundance in two life-cycle stages of *Trypanosoma brucei* and identification of  
58 621 splicing and polyadenylation sites. *Nucleic Acids Res* 38:4946-4957.

59  
60 622 **Singla V, Romaguera-Ros M, Garcia-Verdugo JM, Reiter JF** (2010) Ofd1, a human  
61 623 disease gene, regulates the length and distal structure of centrioles. *Dev Cell* 18:410-424.

- 624 **Spinner L, Pastuglia M, Belcram K, Pegoraro M, Goussot M, Bouchez D, Schaefer DG**  
 1 625 (2010) The function of TONNEAU1 in moss reveals ancient mechanisms of division plane  
 2 626 specification and cell elongation in land plants. *Development* 137:2733-2742.
- 3  
 4 627 **Stephan A, Vaughan S, Shaw MK, Gull K, McKean PG** (2007) An essential quality control  
 5 628 mechanism at the eukaryotic basal body prior to intraflagellar transport. *Traffic* 8:1323-1330.
- 6  
 7 629 **Sunter JD, Benz C, André J, Whipple S, McKean PG, Gull K, Ginger ML, Lukes J** (2015)  
 8 630 Modulation of flagellum attachment zone protein FLAM3 and regulation of the cell shape in  
 9 631 *Trypanosoma brucei* life cycle transitions. *J Cell Sci* 128:3117-3130.
- 10  
 11 632 **Tassin AM, Lemullois M, Aubusson-Fleury A** (2015) *Paramecium tetraurelia* basal body  
 12 633 structure. *Cilia* 5:6.
- 13  
 14 634 **Vaughan S, Gull K** (2015) Basal body structure and cell cycle-dependent biogenesis in  
 15 635 *Trypanosoma brucei*. *Cilia* 5:5.
- 16  
 17 636 **Vaughan S, Kohl L, Ngai I, Wheeler RJ, Gull K** (2008) A repetitive protein essential for the  
 18 637 flagellum attachment zone filament structure and function in *Trypanosoma brucei*. *Protist*  
 19 638 159:127-136.
- 20  
 21 639 **Vedrenne C, Giroud C, Robinson DR, Besteiro S, Bosc C, Bringaud F, Baltz T** (2002)  
 22 640 Two related subpellicular cytoskeleton-associated proteins in *Trypanosoma brucei* stabilize  
 23 641 microtubules. *Mol Biol Cell* 13:1058-1070.
- 24  
 25 642 **Vincensini L, Blisnick T, Bastin P** (2011) 1001 model organisms to study cilia and flagella.  
 26 643 *Biol Cell* 103:109-130.
- 27  
 28 644 **Wehland J, Schroder HC, Weber K** (1984) Amino acid sequence requirements in the  
 29 645 epitope recognized by the alpha-tubulin-specific rat monoclonal antibody YL 1/2. *EMBO J*  
 30 646 3:1295-1300.
- 31  
 32 647 **Wheeler RJ, Scheumann N, Wickstead B, Gull K, Vaughan S** (2013) Cytokinesis  
 33 648 in *Trypanosoma brucei* differs between bloodstream and tsetse trypomastigote forms:  
 34 649 implications for microtubule-based morphogenesis and mutant analysis. *Mol Microbiol*  
 35 650 90:1339-1355.
- 36  
 37 651 **Wickstead B, Ersfeld K, Gull K** (2002) Targeting of a tetracycline-inducible expression  
 38 652 system to the transcriptionally silent minichromosomes of *Trypanosoma brucei*. *Mol Biochem*  
 39 653 *Parasitol* 125:211-216.
- 40  
 41 654 **Woodward R, Carden MJ, Gull K** (1995) Immunological characterization of cytoskeletal  
 42 655 proteins associated with the basal body, axoneme and flagellum attachment zone of  
 43 656 *Trypanosoma brucei*. *Parasitology* 111:77-85.

44 657  
 45 658

## 46 659 **Figure Legends**

48 660 **Figure 1.** Localisation of *TbFOR20*. **(A)** Localisation of YFP::*TbFOR20* at pro- and mature  
 49 661 basal bodies in procyclic *T. brucei*; the main panel images show detection in detergent-  
 50 662 extracted cytoskeletons of YFP::FOR20 distal to the antigen detected by monoclonal  
 51 663 antibody BBA4. The inset shows YFP::FOR20 localises only to basal bodies in intact cells.  
 52 664 6-Diamidino-2-phenylindole (DAPI) was used to detect nuclear DNA (N) and the  
 53 665 mitochondrial genome (or kinetoplast, K) to which pro- and mature basal bodies are  
 54 666 physically attached. **(B)**. YFP::FOR20 localisation in detergent-extracted cytoskeletons in  
 55 667 comparison with the mature basal body antigen(s) detected by monoclonal antibody YL1/2.  
 56 668 **(C)** Duplication of YFP::FOR20 signals coincides with maturation of the existing probasal  
 57 669 body and the biogenesis of new probasal bodies during kinetoplast replication (as denoted  
 58 670 by the 'domed' kinetoplast; Gluenz et al. 2011). **(D)** Localisation of *TbFOR20::myc* at pro-

61  
 62  
 63  
 64  
 65

671 and mature basal bodies in detergent-extracted procyclic *T. brucei*. Formaldehyde fixed  
1 672 cytoskeletons and whole cells (not shown) were decorated for indirect immunofluorescence  
2 673 using anti-myc monoclonal primary antibody. Scale bars in all main panels indicate 5  $\mu$ m and  
3 674 in the inset of (A) 1  $\mu$ m.

5 675

7 676 **Figure 2.** Localisation of *T. brucei* FOP family proteins on isolated flagella. Spatial resolution  
8 677 of indirect immunofluorescence signals for (A) YL1/2 from *TbYFP::FOR20*, (B) polyclonal  
9 678 anti-RP2 from *TbYFP::OFD1*, (C) anti-RP2 from *TbYFP::FOP*, (D) BBA4 and anti-RP2 from  
10 679 *TbYFP::FOR20*, (E) BBA4, anti-RP2, and *TbFOR20::Myc*. Main panel scale bars, 5  $\mu$ m.

13 680

15 681 **Figure 3.** Immunoblot detection of *TbRP2* by monoclonal antibody YL1/2. (A) Detection of  
16 682 *TbRP2* depletion in procyclic *TbRP2* RNAi mutants by immunoblot. The left-hand  
17 683 immunoblot shows detection of both *TbRP2* (predicted mass 50.6 kDa) and tyrosinated  $\alpha$ -  
18 684 tubulin (predicted mass 49.8 kDa) from whole cell extracts ( $2 \times 10^6$  cell equivalents loaded  
19 685 per lane) by YL1/2; proteins were separated by SDS-PAGE using a 10 % polyacrylamide  
20 686 gel. The right-hand immunoblot shows the depletion of *TbRP2* from *TbRP2* RNAi mutants  
21 687 using polyclonal, affinity-purified antibodies raised against recombinant *TbRP2*. Cells were  
22 688 induced for RNAi for 48 h before preparation of cell lysates (RNAi+ lanes). (B) Immunoblot  
23 689 detection of recombinant *TbRP2* by YL1/2; the amount of recombinant protein loaded per  
24 690 lane is indicated; reproduced from André et al. (2014) under the terms of a Creative  
25 691 Common Attribution 3.0 unported licence.

29 692

31 693 **Figure 4.** An N-terminal extension unique to FOR20 proteins from *T. brucei* and closely  
32 694 related African trypanosome species. (A) Evolutionary relationships between trypanosomatid  
33 695 species. (B) Clustal Omega alignment of amino acid sequences for FOR20 orthologues from  
34 696 kinetoplastid protists and other, evolutionary diverse flagellates. Positions of amino acid  
35 697 identity (\*) and conservation (:) are indicated; negatively charged amino acids within the N-  
36 698 terminal extensions of FOR20 from *T. vivax*, *T. congolense*, and *T. brucei* are italicised.  
37 699 'African' trypanosome species are in red; trypanosomatid species more closely related  
38 700 phylogenetically to *T. cruzi* than to the *T. brucei* clade are in purple; other kinetoplastids are  
39 701 in blue. Taxonomic abbreviations: Bs, *Bodo saltans*; Cr, *Chlamydomonas reinhardtii*; Dr,  
40 702 *Danio rerio*; Gg, *Gallus gallus*; Gl, *Giardia lamblia*; Hs, *Homo sapiens*; Lm, *Leishmania*  
41 703 *major*; Ng, *Naegleria gruberi*; Nv, *Nematostella vectensis*; Pt, *Paramecium tetraurelia*; Tb,  
42 704 *Trypanosoma brucei*; Tc, *T. cruzi*; Tcg, *T. congolense*; Tg, *T. grayi*; Tr, *T. rangeli*; Tt,  
43 705 *Tetrahymena thermophila*; Tv, *Trypanosoma vivax*; Tva, *Trichomonas vaginalis*; Xl,  
44 706 *Xenopus laevis*.

47 707

49 708 **Figure 5.** Targeting of trypanosomatid FOR20 to pro- and mature basal bodies in procyclic  
50 709 *T. brucei*. (A) Inducible expression of *TbFOR20 <sup>$\Delta$ 1-21::myc</sup>*: main panel, a formaldehyde-fixed  
51 710 cell decorated for indirect immunofluorescence using anti-myc monoclonal primary antibody;  
52 711 inset, absence of *TbFOR20 <sup>$\Delta$ 1-21::myc</sup>* from detergent-extracted cytoskeletons. (B) Mature  
53 712 basal body localisation only for constitutively expressed *TbFOR20 <sup>$\Delta$ 22-151::RP2 <sup>$\Delta$ 1/ $\Delta$ 134-463::myc</sup></sup>*;  
54 713 panels and merged insets correspond to kinetoplast-basal body regions from 1K1N, 2K1N  
55 714 and 2K2N cells where the mature basal body is decorated by a YFP fusion of the *T. brucei*  
56 715 orthologue of FOP family protein OFD1. (C-D) Localisation of *TcFOR20::myc* at both pro-  
57 716 and mature basal bodies; cells were decorated with anti-myc plus either BBA4 (C) or anti-



717 *Tb*RP2 antibodies (**D**). K, kinetoplast; m, mature basal body; p, probasal body. Scale bars  
1 718 correspond to 5  $\mu$ m (**A-D**) and 1  $\mu$ m (inset **B** and **C-D**).

2  
3 719  
4  
5 720 **Figure 6.** Phyre<sup>2</sup> prediction of *Tb*FOR20 secondary structure. Relative predictions of  
6 721 confidence for disorder and  $\alpha$ -helical regions are indicated. TOF and LisH motifs are known  
7 722 to adopt  $\alpha$ -helical conformations: the *Tb*FOR20 TOF motif spans amino acids 30-60 and the  
8 723 LisH motif amino acids 78-104.

10 724  
11  
12  
13 725 **Figure 7.** Site-directed mutagenesis of *Tb*FOR20 TOF and LisH motifs. (**A**) E37A mutation  
14 726 abrogates protein targeting to the basal/probasal bodies. Main panels show punctate  
15 727 accumulation of protein in whole cells; inset shows the absence of protein from basal body  
16 728 region in detergent extracted cytoskeletons. (**B-C**) Basal body localisation of F54A (B) and  
17 729 Y88A (C) site-directed mutants.

19 730  
20  
21  
22 731 **Figure 8.** Organisation of FOP family proteins at mature trypanosome basal bodies.  
23 732 Positions of FOP family proteins are shown relative to the proximal end antigen recognised  
24 733 by monoclonal antibody BBA4 and TAC component TBCCD1 (an additional tubulin cofactor  
25 734 C domain-containing protein (André et al. 2013)).

27 735  
28  
29 736 **Supplementary Figure 1.** Immunoblot analysis of YFP- and epitope-tagged proteins  
30 737 analysed in this study. Whole cell lysates corresponding to  $2 \times 10^6$  cell equivalents were  
31 738 loaded in all lanes for all panels. (**A**) Constitutive expression of YFP::*Tb*FOR20 (expected  
32 739 molecular mass ~45 kDa). (**B**) Doxycycline-inducible expression of *Tb*FOR20::myc E37A,  
33 740 F54A, and Y88A site-directed mutants; protein levels were determined relative to *Tb*AKF, an  
34 741 adenylate kinase isoform detected using protein-specific polyclonal antisera. (**C**)  
35 742 Doxycycline-inducible expression of *Tb*FOR20::myc (~20 kDa) and *Tb*FOR20 <sup>$\Delta$ 1-21</sup>::myc (~18  
36 743 kDa); -, no doxycycline added; +, doxycycline-dependent induction of gene expression for 24  
37 744 h. (**D**) Constitutive expression of *Tc*FOR20::myc (~18 kDa; lane 2) and *Tb*FOR20 <sup>$\Delta$ 22-</sup>  
38 745 <sup>151</sup>::RP2 <sup>$\Delta$ 1/ $\Delta$ 134-463</sup>::myc (~21 kDa; lane 3); *Tb*FOR20::myc (~20 kDa; lane 1) was  
39 746 immunoblotted for comparison. (**E**) Time-dependent depletion of *Tb*YFP::FOR20 expression  
40 747 in *Tb*FOR20 RNAi mutants. RNAi was induced in cells modified at an endogenous  
41 748 chromosomal location for expression of *Tb*YFP::FOR20; levels of the YFP-fusion protein  
42 749 were determined at the time points indicated, relative to  $\beta$ -tubulin detected by KMx-1  
43 748 monoclonal antibody. Other primary monoclonal antibodies used to probe immunoblots were  
44 749 BB2 (panels A and E, recognising the Ty-epitope engineered into the YFP-fusion) or AbCam  
45 750 anti-myc 9E10 (panels B-D).  
46 751  
47 752  
48 752

49  
50 753

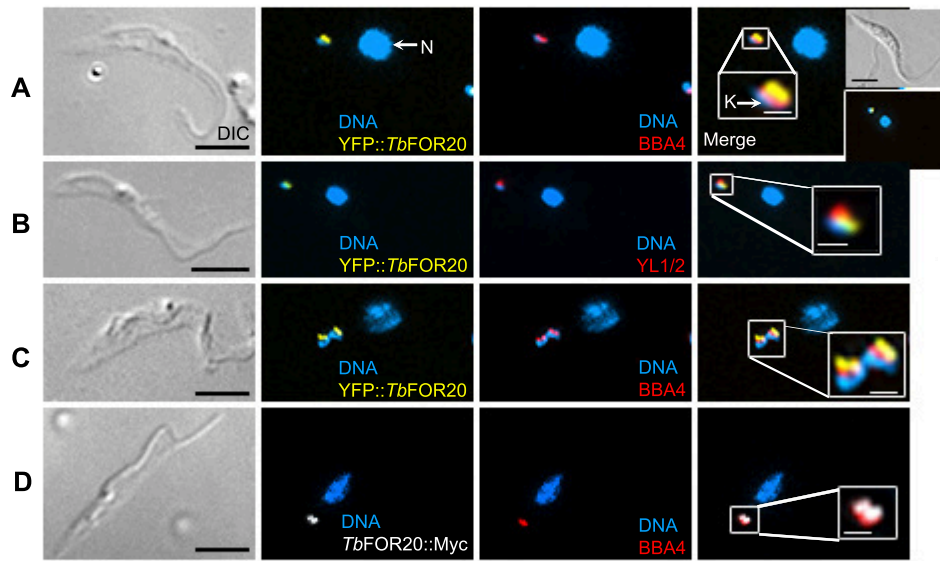


Fig. 1

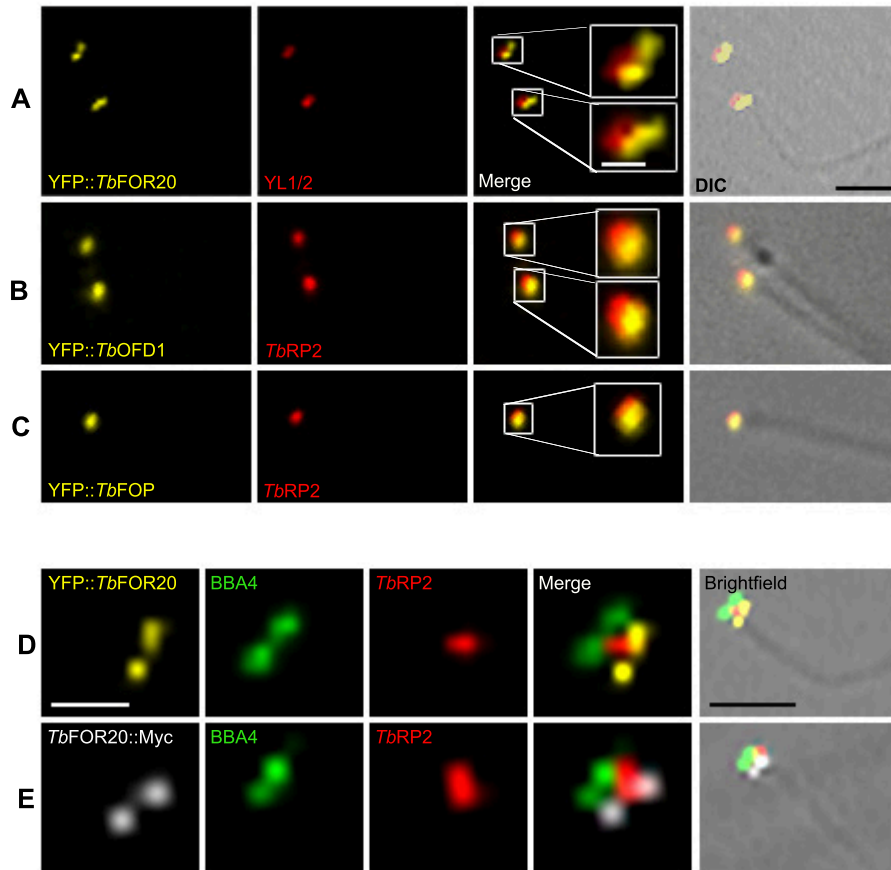


Fig. 2

Figure 3

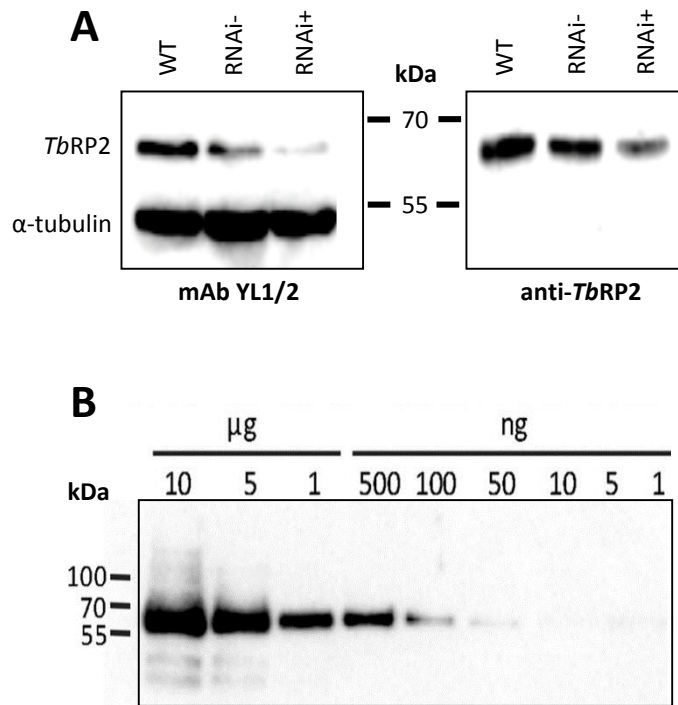
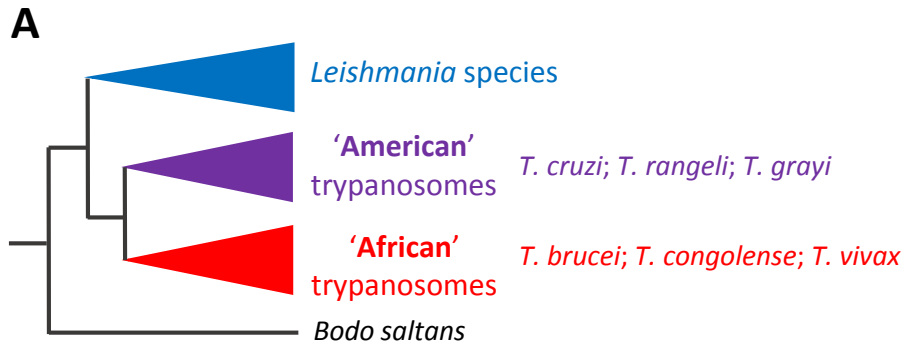


Fig. 3

Figure 4



**B**

<i>Xl</i>	-----MATVGD LKAVVKDTLEKRGVMGQLKARVRAEVFEALDD	38
<i>Gg</i>	-----MATIAELKAVLKDTLEKRGALRQIKARIRAEVFNALDD	38
<i>Hs</i>	-----MATVAELKAVLKDTLEKKGVLGHLKARIRAEVFNALDD	38
<i>Dr</i>	-----MATITELKSALRETLEARGVLGQLKARVRAEVFSALDD	38
<i>Nv</i>	-----MATSSEKLKEVLKETLDNRGILGQIRARIRAEVFSALDD	39
<i>Cr</i>	-----MASVEDLKDALRENLD RSGKLRQLKAQLRADVYNALHN	38
<i>Tt</i>	-----MASVNELKDV LKETLEEKGVLTRIRAKIRAEIFNLND	38
<i>Pt</i>	-----MTFINEMKDALKETLESRGVLSQLRARIRAEIFNLNE	38
<i>Ng</i>	-----MSLEEIKDILKDNLEKRGV LNKIRANLRAEIPKTFEE	37
<i>Gl</i>	-----MDEIKSII LQNMKQRGELAVLQAKVRESVLRALLEG	35
<i>Tva</i>	-----MSVSLGDLND AVVASLRETGKLGQITAQIRAEIYRILTE	39
<i>Tb</i>	MEERE EGEVRRRESFNAP E-ATMSKHGSLKDAMRQVLETKGVIDHVKAELRAAIFHSLQE	59
<i>Tcg</i>	--MEEEDGIPYKFSAPASVAGTTKHGSLKDAMREVLETKGVIDHVKAELRAAIFHSLQE	58
<i>Tv</i>	--MDEPGE-----HPVAPATGVPRQEALKDAMREIMETKGVINHVKAE LRAAIFHSLQE	52
<i>Tc</i>	-----MAMARQESLKEAMREVLETKGVMDHVKAELRAAIFHALQD	40
<i>Tr</i>	-----MTKQESLKEAMREVLETKGVMDHVKAELRAAIFHALQD	38
<i>Tg</i>	-----MSNQESLKGAMREVLEAKGVIDHVKAELRAAIFQSLQD	38
<i>Lm</i>	-----MPNQESLKAAMRDSLEANGTISR IKAELRAAIFERLSD	38
<i>Bs</i>	-----MATNDAAALKAAMRETLENNGQLDNIKAQLRAVVFQALDA	40

:: : : \* : : \* . : \* : :  
TOF domain

Fig. 4

Figure 5

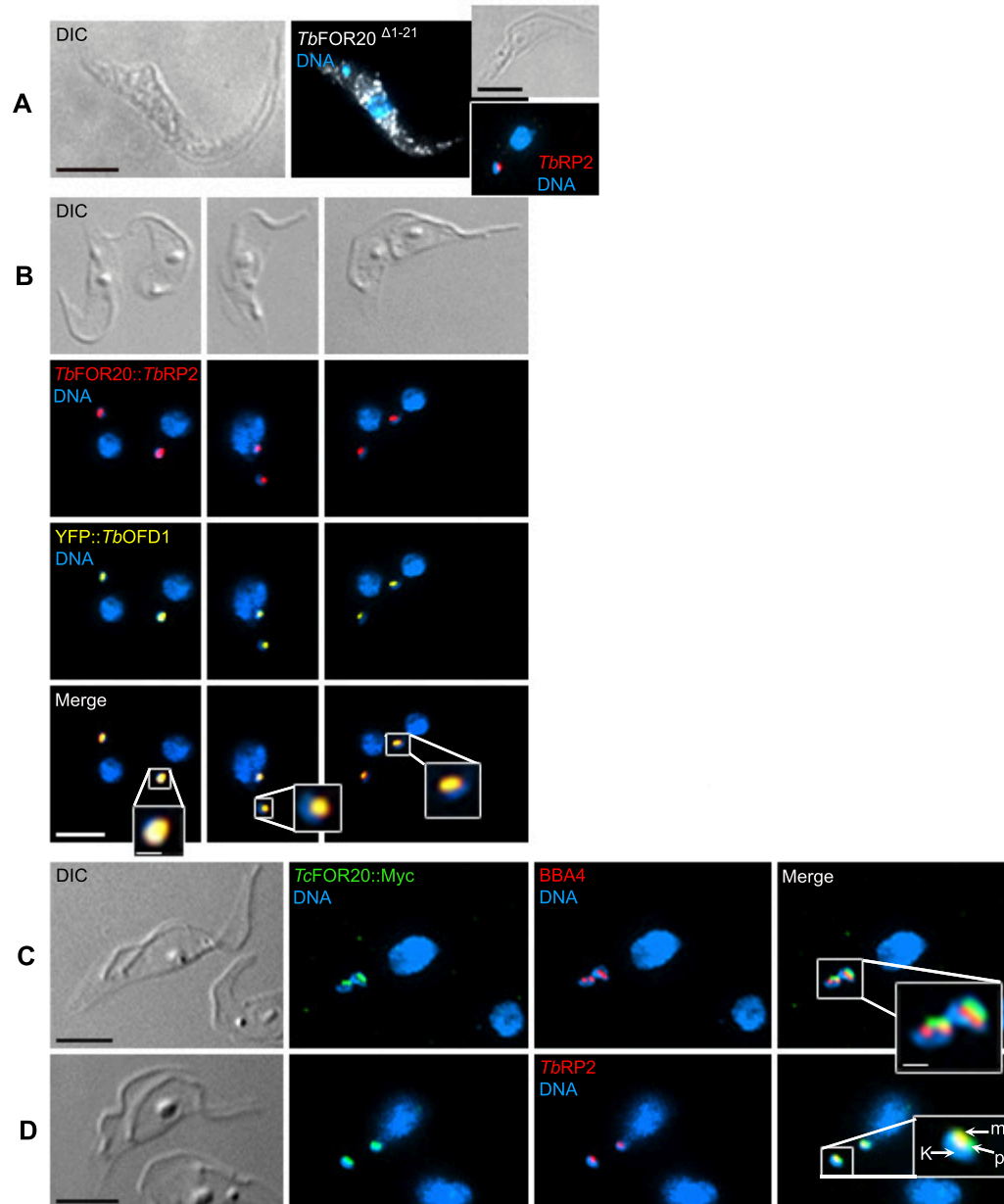


Fig. 5

Figure 6

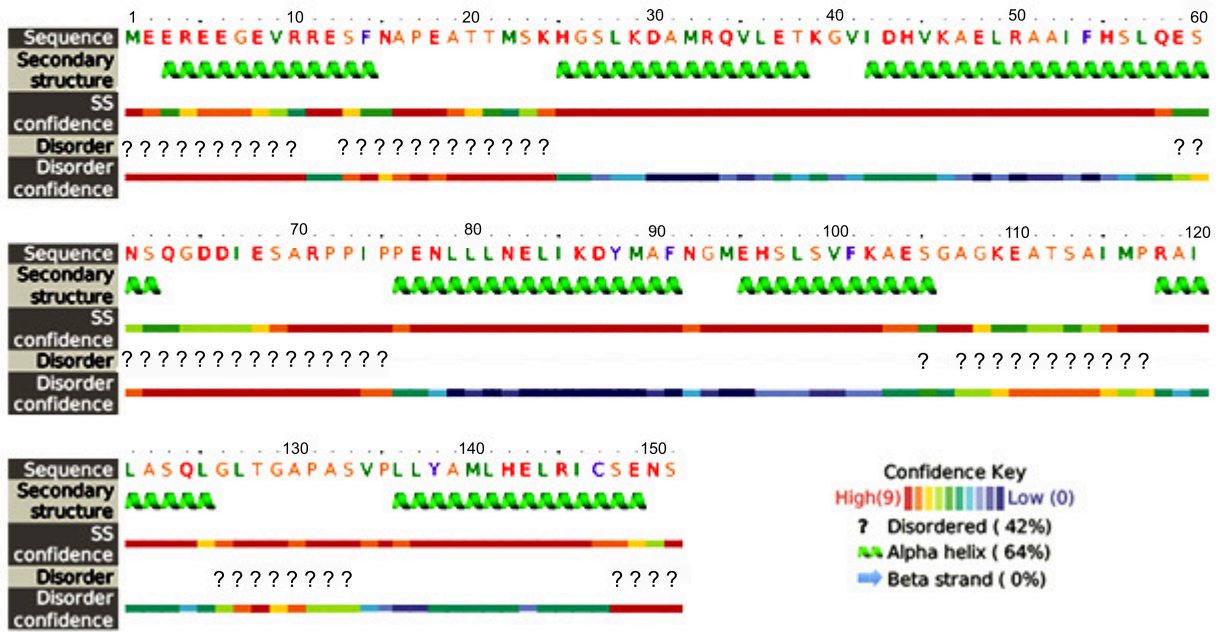


Fig. 6

Figure 7

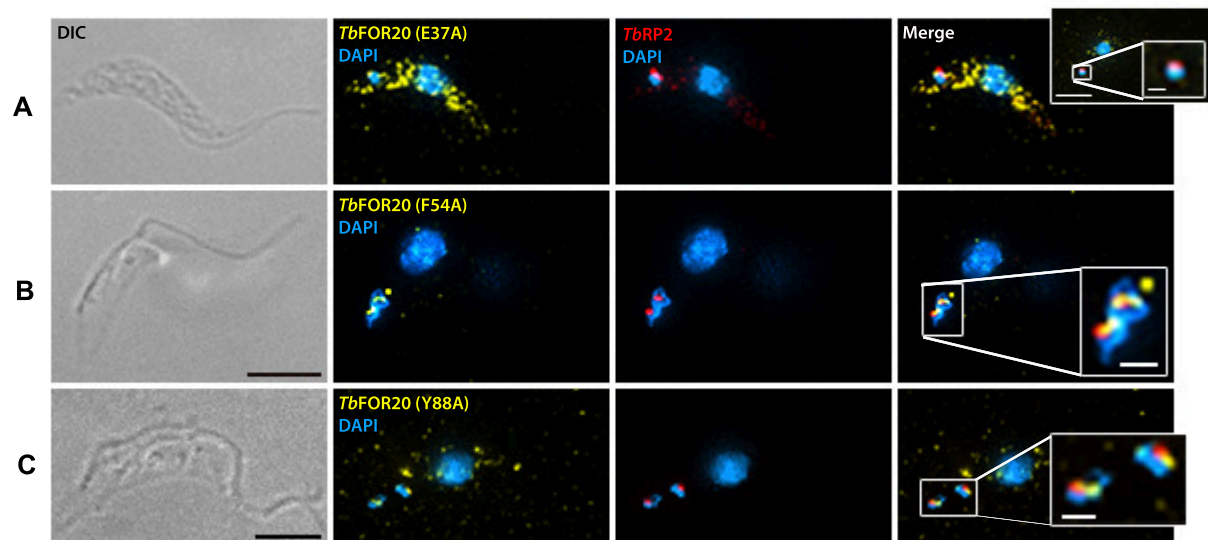


Fig. 7



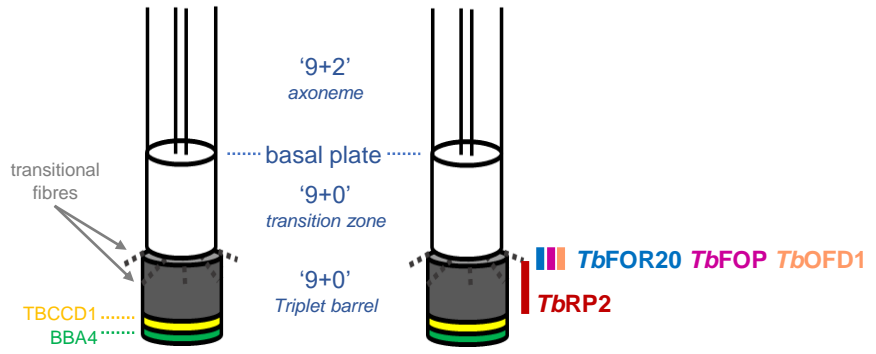


Fig. 8

**Supplement Figure 1**

[Click here to download Supplement Material: for20\\_Supp\\_Fig\\_1.pdf](#)